Available online at www.sciencedirect.com
SCIENCE DIRECT®
Deep-Sea Research I 51 (2004) 1769–1780
DEEP-SEA RESEARCH PART I
www.elsevier.com/locate/dsr

Sedimentation in the Southern Okinawa Trough: enhanced particle scavenging and teleconnection between the Equatorial Pacific and western Pacific margins

Shih-Yu Lee[a,1], Chih-An Huh[a,*], Chih-Chieh Su[a], Chen-Feng You[b]

[a]*Academia Sinica, Institute of Earth Sciences, P.O. Box 1-55, Nankang, Taipei 115, Taiwan, ROC*
[b]*Department of Earth Sciences, National Cheng-Kung University, Tainan, Taiwan, ROC*

Received 11 September 2002; received in revised form 18 March 2004; accepted 15 July 2004
Available online 15 September 2004

Abstract

Owing to its location, geomorphology and hydrodynamic conditions, the southernmost part of the Southern Okinawa Trough (SOT) acts like an efficient receptacle for sediments from Taiwan and the East China Sea shelf. The high sediment flux coupled with the passage, bifurcation, upwelling, swirling and detour of Kuroshio in the SOT area result in intense particle scavenging, with sedimentary inventories of ^{210}Pb and $^{239,\ 240}$Pu far greater than expected from local atmospheric input and in situ water column production. The unusually high inventories, as well as the deposition history of Pu isotopes must be explained by advective transport of Pu westward from the Marshall Islands, the largest source of Pu in the Pacific, by the North Equatorial Current (NEC) followed by northward transport of Kuroshio to the SOT area. The high sedimentation rate in the SOT area enabled us to differentiate the subsurface peak of $^{239,\ 240}$Pu resulting from the global fallout maximum in AD 1963 and the subsurface maximum of ^{240}Pu/^{239}Pu caused by close-in fallout from neutron-rich thermonuclear tests conducted by the US during AD 1952–1954 at the Enewetak and Bikini Atolls. The vertical offset between the subsurface peaks of $^{239,\ 240}$Pu and ^{240}Pu/^{239}Pu in sediments suggests that deposition of the ^{240}Pu/^{239}Pu maximum preceded that of the $^{239,\ 240}$Pu maximum by 3–5 yr and that the transit time of the ^{240}Pu-enriched Pu from its source (at ~12°N, 162°E) to the SOT area is ~6 yr. The mean velocity of NEC thus calculated is ~0.022 m s^{-1}.

The present is the key to the past. This study reveals teleconnection between the Equatorial Pacific and the western Pacific margins and suggests that ODP and IMAGES cores recently collected from the SOT area holds great promise for the reconstruction of high-resolution paleoceanographic records along the trajectories of NEC and Kuroshio.

Keywords: ^{137}Cs; ^{210}Pb; Plutonium isotopes; Okinawa Trough; Kuroshio; North equatorial current

*Corresponding author. Tel.: +886-2-2783-9910; fax: +886-2-2783-9871.
E-mail address: huh@earth.sinica.edu.tw (C.-A. Huh).
[1]Present address: Department of Geological Sciences, University of Michigan, Ann Arbor, MI 48109, USA.

0967-0637/$ - see front matter © 2004 Elsevier Ltd. All rights reserved.
doi:10.1016/j.dsr.2004.07.008

1. Introduction

The sea off northeastern Taiwan is an extremely energetic regime, both tectonically and hydrodynamically. Fig. 1 shows pronounced changes in seafloor morphology and tectonic features off eastern Taiwan, i.e., the south-to-north progression of the Philippine Sea Plate, the Ryukyu Trench, the Ryukyu Arc, the Southern Okinawa Trough (SOT) and the East China Sea continental shelf (for more details, please refer to http://dmc.earth.sinica.edu.tw/Geophysics/twn_topo.html). The Philippine Sea Plate is advancing northwestward at a mean velocity of $\sim 7\,\mathrm{cm\,yr^{-1}}$ (Seno et al., 1993; Lallemand et al., 1997), plunging down the Ryukyu Trench and leading to the Ryukyu volcanic arc in the front and the Okinawa Trough at the back. It is generally thought that the subduction of the Philippine Sea Plate is the mechanism for the active seismic, rifting and

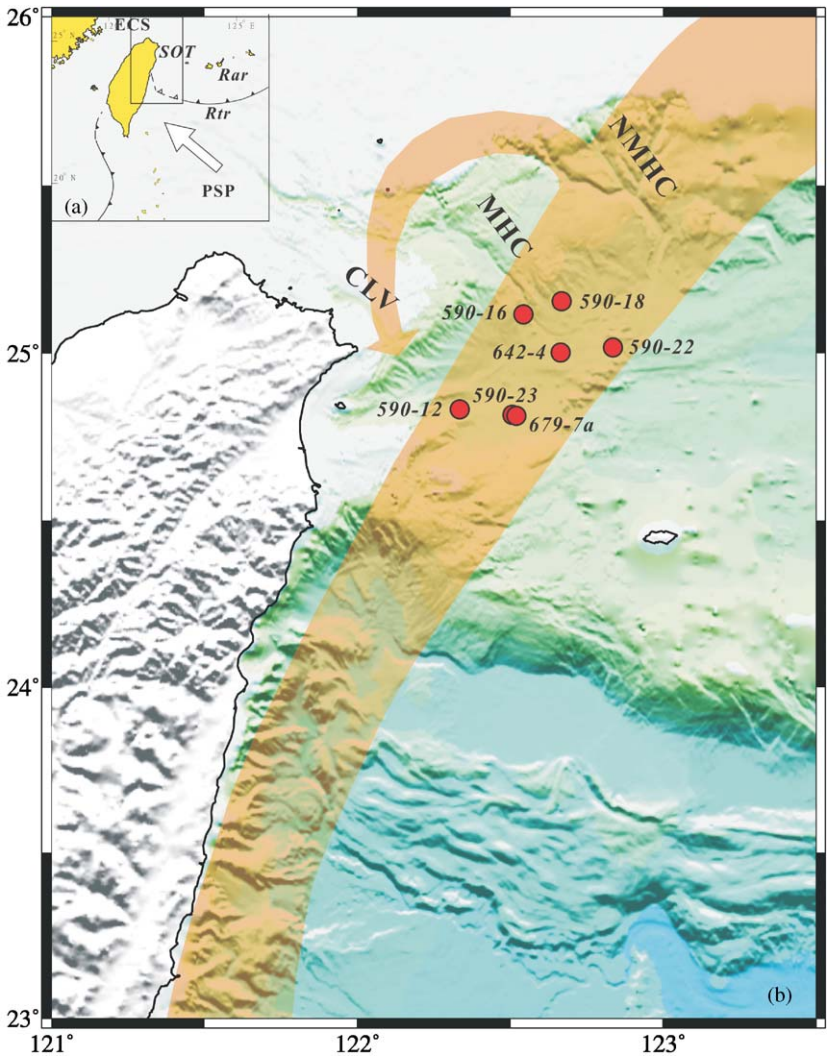

Fig. 1. Map showing (a) the tectonic setting, (b) regional bathymetry and flow path of Kuroshio off eastern Taiwan and over the SOT. Locations of box cores used for this study are also indicated. PSP = Philippine Sea Plate, Rtr = Ryukyu trench, Rar = Ryukyu arc, NMHC = North Mien-Hua Canyon, MHC = Mien-Hua Canyon, CLV = Chilung Valley, ECS = East China Sea.

hydrothermal activities in the Okinawa Trough—a back-arc basin on the making. Crustal activities at this plate boundary are to some extent responsible for the high uplifting and denudation rates of Taiwan, making the island an important source for sediments in this continental margin accretion wedge, as evidenced by high sedimentation rates in the SOT (Lee, 2001).

Concerning hydrodynamic flow in the SOT, this setting is, no doubt, among the most dynamic ones in the world oceans due to the passage of Kuroshio and its interaction with the highly rugged topography. Kuroshio, the western boundary current in the Pacific Ocean, originates from the North Equatorial Current (NEC). As the NEC flows from the east, with its core centered along ~13°N, toward the vicinity of the Luzon Islands, it bifurcates at ~130°E into two branches: Kuroshio toward the north and the Mindanao Current toward the south (Fig. 2). After passing the Luzon Islands and the Bashi Strait, Kuroshio flows in the NNE direction, with its axis lying very close to its western margin and the east coast of Taiwan (see Fig. 1). The volume transport and width of Kuroshio increase on its path from northern Philippine to Taiwan (Nitani, 1972). At 22°N–24°N, Kuroshio is about 300 m deep and 200 km wide, with a maximum velocity between 1 and 2 m s^{-1} near surface and a volume transport between 18 and 25 Sv (Liang et al., 2003). Therefore, it is a major weather machine and conveyor belt, transporting heat, moisture and various chemical materials from low to high latitudes in the western Pacific.

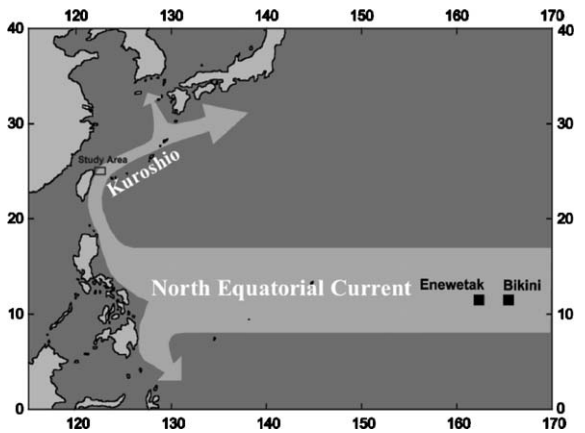

Fig. 2. Schematic chart showing westward flow of the NEC, bifurcation of NEC and northward transport of Kuroshio through the SOT area.

As Kuroshio flows to the northeast of Taiwan, it loses some of its momentum and speed due to collision with the zonally trending East China Sea shelf/slope and bifurcation into two branches. The main stream turns east and flows along the edge of the continental shelf toward Japan, while a branch is topographically steered by the North Mien-Hua Canyon and flows up against the valley into the East China Sea shelf (Fig. 1). This branch then curls back to form a cyclonic eddy centered around the Mien-Hua Canyon with a diameter of ~70 km (Tang and Yang, 1993; Tang et al., 1999). In the center of the eddy, the Kuroshio intermediate water upwells to the surface forming a cold dome. It has been reported that the upwelling and intrusion of Kuroshio onto the continental shelf constitutes the major source for nutrients in the ECS, driving biological productivity in this marginal sea (Chen, 1998). On the other hand, the upwelling and the eddy over the canyon may facilitate offshore and down-slope transport of sediments from the ECS shelf to the Okinawa Trough. Thus, this highly energetic shelf-edge area serves as a conduit or "revolving door" for the exchange of materials between the western Pacific and the East China Sea.

In the backdrop of this complex and dynamic environment are a number of interesting and important marine geochemical, geophysical and paleoceanographic issues that can be addressed. Taking advantage of the proximity of the southernmost end of the SOT to Taiwan, local scientists have used it as a stage to take part in international projects such as Ocean Drilling Program (ODP) and International Marine Past Global Change Study (IMAGES), and to launch regional programs such as Kuroshio Edge Exchange Processes (KEEP) and Long-term Observation and Research of the East China Sea (LORECS). This work is a component of KEEP, whose goal is to study the interactions between Kuroshio and the East China Sea (Wong et al., 2000). Our task was to employ fallout nuclides (^{137}Cs, ^{210}Pb, ^{239,240}Pu) as tracers

to elucidate sedimentation and scavenging processes in the study area. As with our previous works in the vast ECS shelf (Huh and Su, 1999; Su and Huh, 2002), we calculated sedimentation rates from nuclide profiles, thus establishing sediment chronologies and sediment budget. We also evaluated the intensity of particle scavenging based on sedimentary inventories of nuclides. Another focus of this paper is the implications of ICP-MS measured $^{240}Pu/^{239}Pu$ data on the source-to-sink pathways of Pu and, by extension, other particle-reactive chemical species.

Although ^{210}Pb ($T_{1/2} = 22.26$ yr) and the anthropogenic ^{137}Cs and Pu isotopes can be used to derive sedimentation rates and processes on timescales only up to 100 yr, the information obtained from this study has profound implications for other studies in this all-important region. Based on the geological doctrine of uniformitarianism, what is learnt from contemporary sedimentation can be extended backward to unravel the history in the geological past. With this in mind, we had occupied stations not only to fulfill the objective of this study but also to overlap with ODP and IMAGES drilling sites with a view to use the present as a key to the past.

2. Materials and methods

The sediment cores used for this study were taken from water depths over 1000 m (Fig. 1). They were judiciously selected from a large number of box cores collected onboard R/V *Ocean Researcher-I* from three cruises: OR-590 (July 23–27, 2000), OR-642 (April 24–30, 2002) and OR-679 (April 17–24, 2003). In order to focus better on the afore-mentioned issues, we report here cores with fairly constant sedimentation and purposely excluded those containing turbidites, showing unsteady sedimentation and mixing, which have been reported elsewhere (Huh et al., 2004).

The core tops of these cores were well preserved upon recovery as evidenced by transparent bottom water on top of sediments in the box corer. After the overlying water was siphoned out carefully without disturbance of the sediment–water interface, core barrels were inserted into the box to take subcores. Sediments in the core barrels were extruded onboard with a hydraulic jack and sampled at 1–2-cm intervals. The outer rim (~0.5 cm) of each sediment slab was trimmed off to minimize contamination between layers. The sectioned samples were sealed in 8-oz plastic jars and kept frozen until further processing in the home laboratory. Based on weight loss after freeze-drying, water contents of the wet sediments were calculated. A correction for the amount of salt retained in the dry sediments was made based on water content and bottom water salinity. Activities and inventories of nuclides and mass accumulation rates reported in this paper were calculated on salt-free basis.

^{210}Pb (via ^{210}Po) and $^{239,240}Pu$ were first determined by α-spectrometry. ^{209}Po and ^{242}Pu obtained from ORNL were added as the yield determinants prior to total digestion of samples. The ^{209}Po and ^{242}Pu spikes have been calibrated versus NIST-certified ^{208}Po (SRM-4327) and ^{244}Pu (SRM-996), respectively. Polonium isotopes were plated onto a silver disc from the sample solution (in 1.5 N HCl, in the presence of ascorbic acid) at 80–90 °C for 1–2 h. Isotopes of Pu were electroplated onto stainless steel discs. The counting results were corrected for the decay of ^{210}Po (from the time of plating to counting) and ^{210}Pb (from sample collection to Po plating). More detailed description of the radiochemical procedures has been given elsewhere (Huh et al., 1987, 1990, 1996).

^{214}Pb (a precursor of ^{210}Pb, used as an index of supported ^{210}Pb) and ^{137}Cs were measured by γ-spectrometry based on photon energies at 351.99 and 661.62 keV, respectively. The counting system is equipped with a 150% efficiency (relative to 3 × 3 NaI) HPGe detector (EG&G ORTEC GEM-150230) interfaced to a digital gamma-ray spectrometer (DSPec Plus®). The detector was calibrated using NIST SRM 4353 (Rocky Flats soil) and further tuned with IAEA reference materials 133A, 327 and 375. At 661.62 keV, for example, the absolute counting efficiency for our samples (in plastic jars of 8.5-cm diameter, 7-cm height) varied from 6.15% for 10-g samples to 4.66% for 100-g samples, and the peak resolution was 1.21 keV

(FWHM) with a peak-to-Compton ratio higher than 90.

At a later stage of this work, the Pu samples that had been assayed by alpha spectrometry were reprocessed for ICP-MS analysis to obtain the $^{240}Pu/^{239}Pu$ ratio. The procedure entailed removal of the Pu source from the stainless steel plates by leaching with 8N HNO_3, followed by ion exchange operations to remove Fe and traces of other metals inadvertently came off the stainless steel discs along with Pu during acid leaching. Briefly, Pu in the 8 N HNO_3 lechate was purified by passing the solution through an anion column ($AG1 \times 8$), followed by successive washing of the column with an additional amount of 8 N HNO_3 and 9 N HCl to get rid of Fe and other impurities. Pu was then eluted off the column into a Teflon beaker with 1.2 N HCl. After the eluant was evaporated to incipient dryness, Pu was picked up with ~1 ml of 1 N HNO_3 for isotopic analysis on a Finnigan MAT (Bremen, Germany) Element II inductively coupled plasma mass spectrometer. The Element II is a sector field double-focusing mass spectrometer with reverse Neir–Johnson geometry. For Pu isotope measurement, the instrument was operated in low resolution ($m/\Delta m = 300$) with excellent peak flat. The masses at 239, 240 and 242 were integrated for 0.003, 0.040 and 0.003 ms, respectively, and repeated for 600 times. The sample introduction system consisted of a high–stability quartz Scott-type double-pass spray chamber attached with a self-aspirating Teflon MicroFlow nebulizer PFA-50, at a flow rate of ~50 μl min^{-1}.

The precision of the Pu data measured by ICP-MS is comparable to or better than that obtained by alpha spectrometry. The accuracy of the ICP-MS data is ensured by the good agreement with alpha spectrometry data (discussed later) and the analysis of reference material IAEA-327.

3. Results and discussion

Space limitation does not allow us to tabulate the complete dataset, which can be found at the web site http://dmc.earth.sinica.edu.tw/Contributor/Huh/Lee_et_al2004/. For the following discussion, the data are plotted in Fig. 3 to show profiles of ^{137}Cs, excess ^{210}Pb ($^{210}Pb_{ex} = {}^{210}Pb—{}^{214}Pb$), $^{239,240}Pu$ and $^{240}Pu/^{239}Pu$.

It should be noted that Pu was not analyzed for core 590-12 in view of its fast sedimentation rate (see later) and hence inadequate coverage of the ^{137}Cs profile in that core (Fig. 3). If we see ^{137}Cs increases with depth but the subsurface peak representing the 1963 fallout maximum does not emerge within the length (~50 cm) of the core, this most important feature will also be missing for Pu and any bomb-produced nuclides in the core. Thus, insofar as core 590-12 is concerned, it is not justifiable to go through the rather laborious radiochemical procedures for Pu.

3.1. Sedimentation rates

With the combined use of three nuclides as chronometers, we wish to determine sedimentation rates more rigorously. Excess ^{210}Pb profiles in all cores, reported here, show typical exponential decrease with depth (Fig. 3). Sedimentation rates obtained by curve fitting of these profiles generally decrease with increasing distance and water depth offshore, from 1.68 cm yr^{-1} (or 1.40 g cm^{-2} yr^{-1}) in 590-12 to 0.14 cm yr^{-1} (or 0.09 g cm^{-2} yr^{-1}) in 590-22. Note that even the lowest rate measured in our study area is substantially higher than any previously reported sedimentation rates further to the east and north in the Okinawa Trough (Sawada and Handa, 1998; Ujiié and Ujiié, 1999; Jian et al., 2000; Oguri and Matsumoto, 2000). Thus, SOT is apparently an area of focused sedimentation along the path of Kuroshio.

The anthropogenic ^{137}Cs and Pu may be used as independent tracers, based on their known input history in the past 5–6 decades, to further constrain sedimentation rates. The simplest and most widely adopted approach has been the use of the subsurface maximum of these fallout nuclides to mark the time horizon circa AD 1963 , the year with the highest global fallout following a period of most intense atmospheric nuclear tests by the US and, especially, the Former Soviet Union. Such peaks are obvious in all cores except core 590-12 as explained earlier. Sedimentation rates thus

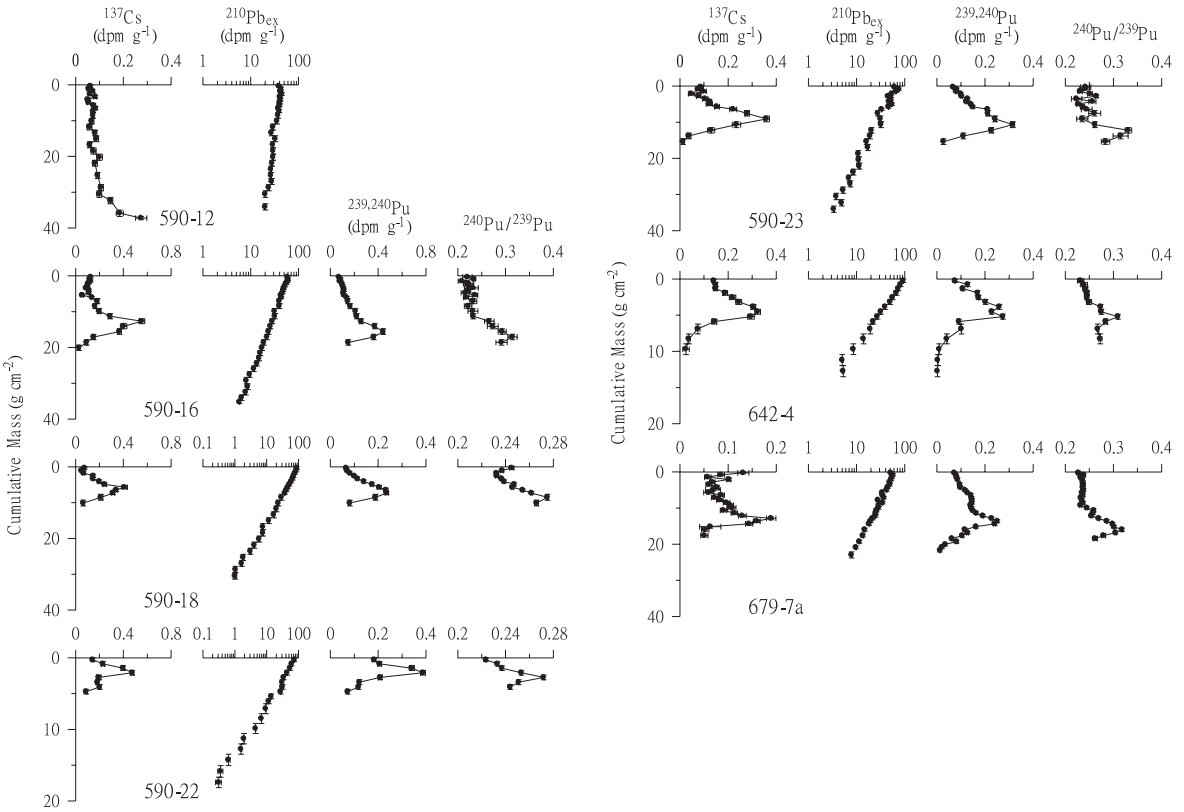

Fig. 3. Profiles of ^{137}Cs, excess ^{210}Pb and $^{239,\ 240}$Pu activities and ^{240}Pu/^{239}Pu atom ratio in the studied cores.

calculated are listed in Table 1 along with ^{210}Pb-based rates for comparison.

Table 1 shows that sedimentation rates derived from $^{210}Pb_{ex}$ and Pu agree very well in all cores except for core 590-22 for which the $^{210}Pb_{ex}$-based rate is greater by ~40%. Core 590-22 has the slowest sedimentation rate among all cores reported here; it is more difficult to attain a sufficient resolution to determine the steep $^{210}Pb_{ex}$ gradient and the shallow depths of the subsurface maximum of ^{137}Cs and Pu. The problem would be further compounded if the core top or sedimentation layers were not flat enough; any sampling artifacts associated with slicing sediment layers not leveled at the top of the core barrel would cause artificial mixing of the sediments and result in disagreement of chronology derived from different tracers.

It is important to note that, when the sedimentation rate is high enough and the sampling resolution is adequate, the Pu peak always lies underneath the ^{137}Cs peak. Consequently, "apparent sedimentation rates" derived from ^{137}Cs tend to be lower. Such a deviation warrants special attention. It could be attributed to the different affinity for particles between ^{137}Cs and Pu. ^{137}Cs is known to be less particle-reactive and therefore it has a longer residence time in seawater, especially when considering that the water column in the study area is more than 1000 m in depth, thus forming a considerable barrier to hinder the arrival of ^{137}Cs at the seafloor. Consequently, the transit time from the surface ocean to eventual deposition at the seafloor is longer for ^{137}Cs relative to Pu, resulting in delayed arrival and therefore a shallower depth of its subsurface maximum in the sediment column. This is quite analogous to the migration of different chemical species at different speeds through an ion-exchange column.

Table 1
Summary of box core location, water depth, sedimentation rates[a] and nuclide inventories[b]

Box core number	Latitude	Longitude	Water depth (m)	Linear sedimentation rate (cm yr^{-1})			Mass accumulation rate (g cm^{-2} yr^{-1})			Nuclide inventory (dpm cm^{-2})		
				$^{210}Pb_{ex}$	^{137}Cs	$^{239,240}Pu$	$^{210}Pb_{ex}$	^{137}Cs	$^{239,240}Pu$	$^{210}Pb_{ex}$	^{137}Cs	$^{239,240}Pu$
590–12	24°49.92′N	122°20.05′E	1184	1.68±0.08	n.a.	n.a.	1.40±0.07	n.a.	n.a.	1995±100	n.a.	n.a.
590–16	25°07.62′N	122°32.78′E	1130	0.64±0.01	0.51±0.03	0.61±0.03	0.47±0.01	0.34±0.02	0.41±0.02	978±21	4.16±0.07	4.05±0.04
590–18	25°10.03′N	122°40.03′E	1282	0.24±0.01	0.20±0.01	0.24±0.01	0.20±0.01	0.15±0.01	0.20±0.01	721±36	2.02±0.04	1.55±0.02
590–22	25°02.04′N	122°50.96′E	1510	0.14±0.01	0.10±0.01	0.10±0.01	0.092±0.003	0.06±0.01	0.06±0.01	285±9	1.21±0.02	1.03±0.01
590–23	24°48.43′N	122°30.30′E	1279	0.44±0.01	0.37±0.03	0.43±0.03	0.35±0.01	0.26±0.02	0.31±0.02	778±22	2.40±0.05	2.59±0.02
642–4	25°00.10′N	122°40.07′E	1474	0.19±0.01	0.19±0.04	0.19±0.04	0.13±0.01	0.12±0.01	0.12±0.01	398±32	1.56±0.03	1.32±0.02
679–7a	24°48.18′N	122°31.04′E	1284	0.48±0.02	0.46±0.03	0.48±0.03	0.36±0.01	0.32±0.01	0.36±0.01	725±20	1.37±0.03	2.44±0.01
									Expected inventory[c]	45–50	6.7	0.21

n.a.: Not analyzed due to inadequate penetration of the box core to the depth marking the 1963 time horizon of global fallout maximum.
[a]^{210}Pb-based rates are derived from exponential curve fitting, while ^{137}Cs- and Pu-based rates are calculated by taking the subsurface peaks as the time horizon circa 1963.
[b]$^{210}Pb_{ex}$ inventories are calculated from the best-fit equations, while ^{137}Cs and Pu inventories are calculated by integrating their activities downcore.
[c]Inventory expected from local atmospheric input (for all three nuclides) plus in situ production from seawater ^{226}Ra in the case for ^{210}Pb.

In summary, based on the good agreement between $^{210}Pb_{ex}$- and Pu-derived sedimentation rates, we believe that sediment mixing is minimal and these two nuclides can complement each other to yield a reliable sediment chronology in this particular environment. However, the efficacy of ^{137}Cs as a time marker cannot be overlooked, especially when we consider that ^{137}Cs can be more easily measured by the non-destructive gamma spectrometry.

3.2. Nuclide inventories: enhanced particle scavenging of ^{210}Pb and Pu in the SOT

By integrating nuclide activities (dpm g^{-1}) with cumulative mass (g cm^{-2}) downcore, nuclide inventories (dpm cm^{-2}) in sediments are calculated. The results are also summarized in Table 1. It would be informative to compare the observed inventories against cumulative fallout expected from atmospheric input and in situ production of ^{210}Pb from seawater ^{226}Ra. In a previous study concerning the East China Sea, such "overhead" reference values were estimated to be 0.21, 7.1 and 60 dpm cm^{-2} for Pu, ^{137}Cs and ^{210}Pb, respectively (Huh and Su, 1999). Considering the geographic proximity, we would expect similar Pu and ^{137}Cs fluxes from global fallout in the SOT area. However, since 2–5 yr has elapsed, the reference value for ^{137}Cs should be decay corrected from 7.1 dpm cm^{-2}, as of January 1998 for the previous work, to 6.8 dpm cm^{-2}, as of July 2000, and 6.3 dpm cm^{-2}, as of July 2003, for this study. As regards ^{210}Pb, its flux is highly dependent on land–sea distribution, precipitation, and water column production, which are fairly different between the ECS shelf and the SOT area. Therefore, it is necessary to make a site-specific assessment here. For atmospheric flux of ^{210}Pb, we would take 1.06 dpm cm^{-2} yr^{-1} (Su et al., 2003) based on a continuous 5-yr record at Peng-Chia-Yu (25°37.768′N, 122°04.327′E), a nearby islet in the northwest of the study area. For in situ production of ^{210}Pb, the flux calculated for a water column of 1130–1510 m with a mean ^{226}Ra concentration of 0.1 dpm l^{-1} (Yeh and Chung, 1997) is 0.35–0.50 dpm cm^{-2} yr^{-1}. Thus, the total ^{210}Pb input to the water column amounts

to 1.41–1.56 dpm cm^{-2} yr^{-1}, which could sustain a sedimentary ^{210}Pb inventory up to 45–50 dpm cm^{-2} at steady state.

Compared with the reference values recapitulated above (namely, 0.21, 6.3–6.8 and 45–50 dpm cm^{-2} for Pu, ^{137}Cs and $^{210}Pb_{ex}$, respectively), the observed inventories of $^{210}Pb_{ex}$ and Pu are about 5–20 times higher than expected and correlate positively to sedimentation rate. So, there must exist additional input terms for Pu and ^{210}Pb in the study area. Potential sources for the extra Pu and ^{210}Pb inventories in the study area include: (1) sediments exported across the ECS shelf, (2) drainage basin input from eastern Taiwan, and (3) lateral input of open ocean water in conjunction with enhanced particle scavenging in the SOT area. The relative importance of these possible sources is evaluated below.

It was hypothesized during the KEEP project that the SOT area constitutes a sink for sediments from the ECS shelf (Wong et al., 2000). Sediment traps deployed on the slope region between the ECS shelf and the SOT area did capture time-averaged mass fluxes as high as ~2 g cm^{-2} yr^{-1} and that the sediment particles were transported primarily through canyons, not across the slope area (Chung and Hung, 2000). From the spatial pattern of sediment trap-measured mass flux, it is suggested that most of the sediments transported down the canyon did not reach the trough directly. Rather, before reaching the base of the slope, the sediments were entrained and transported by a year-round undercurrent over the slope flowing toward the southwestern end of the basin (Chung and Hung, 2000; Liang et al., 2003). This is consistent with our observation that sedimentation rates at site 590-16 down the Mien-Hua Canyon and elsewhere down the ECS slope are much less than that at site 590-12 in the west.

Although the ECS shelf may be an important source of sediments to the SOT, it is probably less important as a source of fallout nuclides in the SOT area in view of the distinct difference in grain size and ^{210}Pb activity, as explained below. Surficial sediments in the outer shelf of the south ECS, as well as sediment-trap collected particles over the ECS slope and canyons are primarily sand and silt with $^{210}Pb_{ex}$ activities, 1 to 2 orders of magnitude lower than those in surficial sediments (predominantly of clay size) in our study area. Although sediments in the deep SOT are primarily transported from the west, some of them may originate from suspended particles carried to the west by the undercurrent mentioned above. When such particles settle to the deep SOT sediments, they scavenge additional amounts of $^{210}Pb_{ex}$ and Pu from the water column.

With an average annual sediment discharge of 8 million tons per year since 1949 (Water Resources Bureau, 1999), the Langyang River in the northeast of Taiwan is obviously an important source of sediments to the SOT area. The spatial pattern of $\delta^{13}C$ and grain size distribution (please see supplemental material at http://dmc.earth.sinica.edu.tw/Contributor/Huh/Lee_et_al2004/) suggests a pronounced terrestrial plume from the river's estuary and delta toward the SOT area. Could the Langyang River be capable of contributing significantly to the ^{210}Pb budget in the SOT area? We believe the possibility can be ruled out based on the following considerations. The area of the Langyang River's drainage basin is 979 km^2, somewhat less than the seafloor area surrounded by the studied cores (~1000 km^2). Even if we make an extreme (and unrealistic) assumption that the residence time of fallout ^{210}Pb in the drainage basin of Langyang River is nil (i.e., completely exported to the sea), the river is still a relatively small source for fallout nuclides in the SOT area. By analogy, the role of the Langyang River in contributing Pu to the SOT area is also unimportant. This leaves particle scavenging as the process mainly responsible for the observed ^{210}Pb and Pu inventories in SOT sediments, as elaborated below.

The passage of Kuroshio through the SOT area is capable of introducing enormous amounts of particle-reactive chemical species, including ^{210}Pb, Pu and ^{137}Cs, from the open Pacific for removal in the SOT area. Conceivably, the scavenging effect can be intensified by the collision of Kuroshio onto the northern wall of the Okinawa Trough, upwelling of the Kuroshio subsurface water followed by the formation of a cyclonic eddy, and bountiful supply from the Langyang River and the ECS shelf of sediments as scavengers of

particle-reactive materials. The potential of Kuroshio as a source for ^{210}Pb and Pu to the SOT area can be roughly estimated below.

The study area falls well within the path of Kuroshio and is close to its main axis (Fig. 1). With a mean Kuroshio volume transport of ~15 Sv (1 Sv = 10^6 m^3 s^{-1}) in the study area (Liang et al., 2003) and given an average ^{210}Pb concentration of 120 dpm m^{-3} in Kuroshio water (Lin and Chung, 1991), this western boundary current could provide an advective ^{210}Pb flow of 1.8×10^9 dpm s^{-1} (or 5.7×10^{16} dpm yr^{-1}). Dividing this throughput by the area bordered by the core sites (i.e., 1000 km^2) yields 5.7×10^3 dpm cm^{-2} yr^{-1}, which is 90–640 times the vertical flux required to sustain the observed sedimentary ^{210}Pb inventories at steady state. In other words, it requires the removal of merely 0.16–1.1% of the ^{210}Pb advected through the SOT area to account for the observed sediment budget of ^{210}Pb. If a similar calculation is performed for Pu, assuming a mean Pu concentration of 1.2 dpm m^{-3}, in Kuroshio water (Nagaya and Nakamura, 1992) since AD 1963, the total throughput of Pu in the water column overlying the study area during the past four decades would amount to $\sim 1.9 \times 10^{16}$ dpm. Dividing this amount by the area yields 1.9×10^3 dpm cm^{-2}, which is more than 300 times higher than the observed Pu inventories above the subsurface Pu peaks in the studied cores. Thus, the sedimentary budget of Pu in the study area can be easily explained by removing not more than 0.4% of the Pu in Kuroshio water advected through the study area. This is consistent with the calculation based on ^{210}Pb.

In contrast to the large surplus of Pu and ^{210}Pb, the measured ^{137}Cs inventories in sediments (1.2–4.2 dpm cm^{-2}) are substantially lower than its reference value (6.3–6.8 dpm cm^{-2}), again reflecting this nuclide's lower affinity for particles and longer residence time in the water column.

3.3. Downcore distribution of ^{240}Pu/^{239}Pu—implications for sources, pathways and transit time of Pu

As mentioned earlier, following the alpha spectrometric analysis of ^{239,240}Pu, we reprocessed the Pu sources for isotopic analysis by ICP-MS, except for 679-7a, the last core studied, for which Pu isotopes were directly measured by ICP-MS. Fig. 4 shows that the ^{239,240}Pu data, calculated by adding up ^{239}Pu and ^{240}Pu, measured by ICP-MS agree very well with the alpha-spectrometric ^{239,240}Pu data.

Downcore profiles of ^{240}Pu/^{239}Pu (Fig. 3) show the following features. First, at all depths in all cores, ^{240}Pu/^{239}Pu ratios are consistently above 0.22, averaging ~0.26 throughout the cores. These ratios are considerably higher than the average ratio of 0.176 in global fallout reported by Krey et al. (1976). Secondly, as with $^{239,\ 240}$Pu, the ^{240}Pu/^{239}Pu ratio generally increases with depth toward a subsurface maximum. Thirdly, and most interestingly, the ^{240}Pu/^{239}Pu peak is located below the $^{239,\ 240}$Pu peak in all cores except 590-22 in which they reside in the same sampling interval. We believe it is due to the lowest sedimentation rate of 590-22 (hence inadequate sampling resolution) among the studied cores that the ^{240}Pu/^{239}Pu and $^{239,\ 240}$Pu peaks are not separable in that core.

Since sedimentation rates of the studied cores span a wide range, it is not straightforward to compare the offset in depth between the ^{239,240}Pu and the ^{240}Pu/^{239}Pu subsurface peaks among the

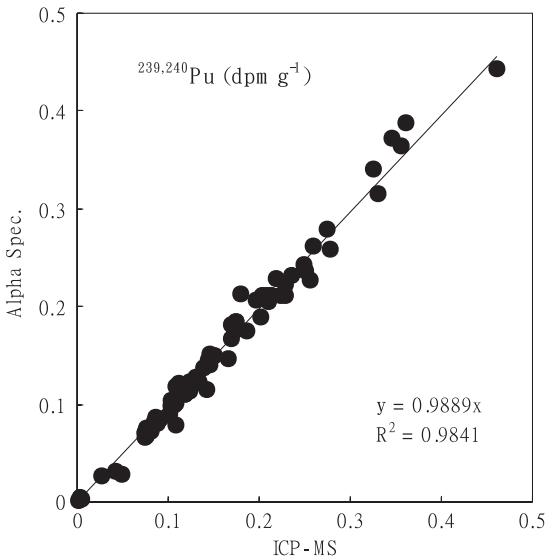

Fig. 4. Correlation between alpha spectrometry and ICP-MS measured $^{239,\ 240}$Pu activities.

cores. An alternative attempt was made to distinguish their arrival times. By setting the fallout $^{239,\ 240}$Pu maximum at AD 1963, we calculated the arrival time of the ^{240}Pu/^{239}Pu maximum based on each individual core's sedimentation rates. The results show that the ^{240}Pu/^{239}Pu maximum falls within the time period from AD 1955 to 1963. If the ^{240}Pu/^{239}Pu versus time plots of all cores are pooled together, and mean ^{240}Pu/^{239}Pu ratios (and standard deviation) are calculated year-by-year to generate a composite plot, the ^{240}Pu/^{239}Pu maximum can be constrained better, as revealed in Fig. 5. Also shown in Fig. 5 for comparison is the single plot for core 679-7a, which was collected and analyzed at a later time with the purpose of improving the time resolution in mind. It was collected from a site with a suitable sedimentation rate and sampled at 1-cm intervals throughout the length of the core. The high-resolution data from a single core does corroborate the composite plot, lending strong support to the validity of the dataset and the following arguments.

These high ^{240}Pu/^{239}Pu ratios and their timing must be ascribed to high-yield, neutron-rich US tests conducted during AD 1946–1958 on the Marshall Islands, which was by far the largest point source for Pu in the Pacific (Robison and Noshkin, 1999). Especially noteworthy are two exceptionally large detonations: the Ivy–Mike shot (10.4 m) on Oct. 31, 1952 at Enewetak Atoll and the Castle–Bravo shot (15 m) on Feb. 28, 1954 at Bikini Atoll. Together, these two shots contributed to more than 90% of the global total yield during

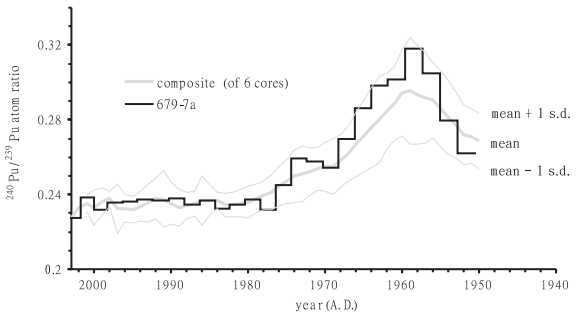

Fig. 5. Plot of ^{240}Pu/^{239}Pu versus time for core 679-7a compared with a composite plot of six cores.

AD 1952–1954. (Carter and Moghissi, 1977). The Ivy–Mike shot produced ^{240}Pu/^{239}Pu ratios of 0.36 (Diamond et al., 1961), and the Bravo shot should yield similarly high ^{240}Pu/^{239}Pu ratios, although no measurements were reported for that shot (Bertine et al., 1986). It is generally accepted that close-in fallout from US Pacific nuclear tests is responsible for the $^{239,\ 240}$Pu inventories in the water column, which are substantially higher than expected from global fallout (Bowen et al., 1980; Livingston et al., 2001). Likewise, close-in fallout will also affect the ^{240}Pu/^{239}Pu ratios in the environment, shifting the values away from the value (~0.18) typical of worldwide fallout.

The highest ^{240}Pu/^{239}Pu ratio we measured, ~0.33, found in BC23 at 16–18 cm depth (Fig. 4), is rather close to the ratio (~0.36) resulting from the Ivy–Mike shot in 1952, suggesting the dominance of high-yield close-in fallout and very rapid transport relative to the residence time of Pu in seawater. The influence of this source to the northwest Pacific Ocean, in general, and to the SOT area, in particular, can be better realized by considering the transport pathway of materials in relation to circulation pattern in the western Pacific. Located near 12°N, Bikini and Enewetak Atolls are right in the path of the NEC (Fig. 2). Hence, Pu derived from these atolls or the nearby waters can be transported by the current to the SOT area, which is an effective sink of sediments and particle-reactive materials. Following the ^{240}Pu/^{239}Pu maximum, the ratios decreased generally toward the core tops to values consistent with recent ^{240}Pu/^{239}Pu ratios in the water column near Bikini Atoll (Bertine et al., 1986). An attempt was made to estimate the transit time from the source (at ~12°N, 163°E) to the sink in the SOT area, as described below.

Fig. 5 indicates that the ^{240}Pu/^{239}Pu peak arrived the SOT area circa AD 1958–1960. A transit time of ~6 yr (since AD 1952–1954) is thus suggested for the transport of the ^{240}Pu-enriched Pu from the Pacific Atolls to the SOT area. The traveling distance of NEC (centered along ~12°N) from the Marshall Islands (~163°E) to the east of Philippine (~125°E) is ~4100 km, and that of Kuroshio along the western Pacific margin from 12°N to 25°N is ~1500 km. Assuming 0.6 m s^{-1} as

the mean velocity of the core of Kuroshio from 12°N to 25°N and above 300 m (Tang et al., 2000), the traveling time of Kuroshio through this segment is not more than a month, very short relative to 6 yr. Thus, the mean velocity at which Pu is transported along NEC can be estimated to be $\sim 0.022\,m\,s^{-1}$. Considering various uncertainties involved, this result compares reasonably well with the annual mean velocity of NEC above 400 m (~ 0.02–$0.06\,m\,s^{-1}$) calculated by Donguy and Meyers (1996) based on XBT data and the climatological temperature–salinity relationship.

4. Conclusions

In conjunction with high sediment flux, the collision of Kuroshio onto the slope of the East China Sea shelf and the topographically steered upwelling, eddy formation and diversion of this western boundary current cause extremely intense scavenging of particle-reactive chemical materials in the SOT area. Seven sediment cores collected from the SOT area were analyzed for ^{137}Cs, ^{210}Pb and Pu isotopes to elucidate sedimentation, chemical scavenging and sources and pathways of nuclides. From the results the following conclusions can be drawn:

(1) With sedimentation rates substantially higher than those observed elsewhere in the Okinawa Trough along the route of Kuroshio, the SOT area is probably the most effective sink of sediments off the East China Sea continental shelf.
(2) The high sedimentation rates in the SOT area offer a very favorable condition for the preservation of paleoceanographic and paleoclimate records in the sediments. Thus, the ODP and IMAGES cores recently recovered from this area are expected to reveal the history of the sedimentation environment at unprecedented high resolution.
(3) Due to high sediment flux, massive passage of open-ocean water and interaction of the Kuroshio water with the continental margin topography, extremely intense scavenging of particle-reactive chemical species takes place in the SOT area, resulting in sedimentary inventories of $^{210}Pb_{ex}$ and $^{239,240}Pu$ far greater than expected from local atmospheric input and water column production (i.e., if there were no Kuroshio flowing through).
(4) Downcore profiles of $^{240}Pu/^{239}Pu$ are characterized by a subsurface maximum underneath the $^{239,240}Pu$ peak, suggestive of Pu input from high-yield neutron-rich nuclear tests in the Pacific prior to AD 1963. Based on the sedimentation rates, the vertical offset between the $^{240}Pu/^{239}Pu$ and $^{239,240}Pu$ peaks, and the circulation pattern in the western Pacific, it is rather certain that the high $^{240}Pu/^{239}Pu$ ratios are derived from thermonuclear tests conducted by the US in the Marshall Islands during the early 1950s. The source-to-sink traveling velocity, estimated from the spatial distance and the elapsed time, supports the notion that NEC and Kuroshio are responsible for the teleconnection between the Equatorial Pacific and the western Pacific margins.

Acknowledgments

We wish to thank Dr. Men-Dar Lee for assistance in the ICP-MS analysis and Dr. Wen-Tzong Liang for data management. This work is supported by the National Science Council Grants NSC90-2611-M-001-002, 91-2611-M-001-002, 92-2611-M-001-002, and 93-2611-M-001-002.

References

Bertine, K.K., Chow, T.J., Koide, M., Goldberg, E.D., 1986. Plutonium isotopes in the environment: some existing problems and some new ocean results. Journal of Environmental Radioactivity 3, 189–201.

Bowen, V.T., Nochkin, V.E., Livingston, H.D., Volchok, H.L., 1980. Fallout radionuclides in the Pacific Ocean: vertical and horizontal distribution, largely from GEOSECS stations. Earth and Planetary Science Letters 49, 411–434.

Carter, M.W., Moghissi, A.A., 1977. Three decades of nuclear testing. Health Physics 33, 55–71.

Chen, C.-T.A., 1998. The Kuroshio intermediate water is the major source of nutrients on the East China Sea continental shelf. Oceanologica Acta 21, 713–716.

Chung, Y.-C., Hung, G.-W., 2000. Particulate fluxes and transports on the slope between the southern East China Sea and the South Okinawa Trough. Deep-Sea Research Part I 20, 571–597.

Diamond, H., Fields, P.R., Stevens, C.S., Studier, M.H., Fried, S.M., Inghram, M.G., Hess, P.C., Pyle, G.L., Mech, J.F., Manning, W.R., Ghiorso, A., Thompson, S.G., Higgins, G.H., Seaborg, G.T., Browne, C.I., Smith, H.L., Spence, R.W., 1961. Heavy isotope adundance in 'Mike' thermonuclear device. Physical Review 119, 2000–2004.

Donguy, J.R., Meyers, G., 1996. Mean annual variation of transport of major currents in the tropical Pacific Ocean. Deep-Sea Research Part I 43, 1105–1122.

Huh, C.-A., Su, C.-C., 1999. Sedimentation dynamics in the East China Sea elucidated from ^{210}Pb, ^{137}Cs and ^{239,240}Pu. Marine Geology 160, 183–196.

Huh, C.-A., Zahnle, D.L., Small, L.F., Noshkin, V.E., 1987. Budgets and behaviors of uranium and thorium series isotopes in Santa Monica Basin sediments. Geochimica et Cosmochimica Acta 51, 1743–1754.

Huh, C.-A., Small, L.F., Niemnil, S., Finney, B.P., Hickey, B.M., Gorsline, D.S., Williams, P.M., 1990. Sedimentation dynamics in the Santa Monica-San Pedro Basin off Los Angeles: radiochemical, sediment trap and transmissometer studies. Continental Shelf Research 10, 137–164.

Huh, C.-A., Chu, K.-S., Wei, C.-L., Liew, P.-M., 1996. Lead-210 and plutonium fallout in Taiwan as recorded at a subalpine lake. Journal of Southeast Asian Earth Science 14, 373–376.

Huh, C.-A., Su, C.-C., Liang, W.-T., Ling, C.-Y., 2004. Linkages between turbidites in the southern Okinawa Trough and submarine earthquakes. Geophysical Research Letters 31, L12304.

Jian, Z., Wang, P., Saito, Y., Wang, J., Pflaumann, U., Oba, T., Cheng, X., 2000. Holocene variability of the Kuroshio Current in the Okinawa Trough, northwestern Pacific Ocean. Earth and Planetary Science Letters 2000, 305–319.

Krey, P.W., Hardy, E.P., Pachuchi, C., Rourke, F., Coluzza, J., Benson, W.K., 1976. Mass isotopic composition of global fall-out plutonium in soil. Proceedings of a Symposium on Transuranium Nuclides in the Environment, IAEA-SM-199-39, 39, pp. 671–678.

Lallemand, S., Liu, C.-S., Font, Y., 1997. A tear fault boundary between the Taiwan orogen and the Ryukyu subduction zone. Tectonophysics 274, 171–190.

Lee, S.-Y., 2001. Sedimentation dynamics off Northeastern Taiwan elucidated from fallout nuclides. M.S. Thesis, National Taiwan University, p. 63 (in Chinese with English abstract).

Liang, W.-D., Tang, T.-Y., Yang, Y.-J., Ko, M.-T., Chuang, W.-S., 2003. Upper-ocean currents around Taiwan. Deep-Sea Research II 50, 1085–1105.

Lin, Y.-N., Chung, Y., 1991. Pb-210 and Po-210 distributions and their radioactive disequilibria in the Kuroshio waters off eastern and northeastern Taiwan. Terrestrial, Atmospheric and Oceanic Sciences 2, 243–265.

Livingston, H.D., Povinec, O.P., Ito, T., Togawa, O., 2001. The behavior of plutonium in the Pacific Ocean. In: Kudo, A. (Ed.), Plutonium in the Environment. Proceedings of the Second Invited International Symposium, November 9–12, 1999. Elsevier, Osaka, Japan, pp. 267–292.

Nagaya, Y., Nakamura, K., 1992. ^{239,240}Pu and ^{137}Cs in the East China and the Yellow Seas. Journal of Oceanography 48, 23–35.

Nitani, H., 1972. In: Stommel, H., Yoshida, K. (Eds.), Beginning of the Kuroshio. University of Tokyo, Kuroshio, pp. 129–163.

Oguri, K., Matsumoto, E., 2000. Evidence for the offshore transport of terrestrial organic matter due to the rise of sea level: the case of the East China Sea continental shelf. Geophysical Research Letters 27 (23), 3893–3896.

Robison, W.L., Noshkin, V.E., 1999. Radionuclide characterization and associated dose from long-lived radionuclides in close-in fallout delivered to the marine environment at Bikini and Enewetak Atolls. The Science of the Total Environment. Special Issue. The Marine Environment—Understanding and Predicting for the Future 237/238, 311–328.

Sawada, K., Handa, N., 1998. Variability of the path of the Kuroshio ocean current over the past 25,000 years. Nature 392, 592–595.

Seno, T., Stein, S., Gripp, A.E., 1993. A model for the motion of the Philippine Sea plate consistent with the NUVEL-1 and geologic data. Journal of Geophysical Research 98 (B10), 17941–17948.

Su, C.-C., Huh, C.-A., 2002. ^{210}Pb, ^{137}Cs and ^{239,240}Pu in East China Sea sediments: sources, pathways and budgets of sediments and radionuclides. Marine Geology 183, 163–178.

Su, C.-A., Huh, C.-A., Lin, F.-J., 2003. Factors controlling atmospheric fluxes of ^{7}Be and ^{210}Pb in northern Taiwan. Geophysical Research Letters 30 (19), 2018.

Tang, T.-Y., Yang, Y.-C., 1993. Low frequency current variability on the shelf break northeast of Taiwan. Journal of Oceanography 49, 193–210.

Tang, T.-Y., Hsueh, Y., Yang, Y.-J., Ma, J.C., 1999. Continental slope flow northeast of Taiwan. Journal of Physical Oceanography 29, 1353–1362.

Tang, T.-Y., Tai, J.-H., Yang, Y.-C., 2000. The flow pattern north of Taiwan and the migration of the Kuroshio. Continental Shelf Research 20, 349–371.

Ujiié, H., Ujiié, Y., 1999. Late Quaternary course changes of the Kuroshio Current in the Ryukyu Arc ridge, northwestern Pacific Ocean. Marine Micropaleontology 37, 23–40.

Water Resources Bureau, 1999. Hydrological Year Book of Taiwan, ROC, 1998.

Wong, G.T.F., Chao, S.-Y., Li, Y.-H., Chung, Y.-C., 2000. KEEP—exchange processes between the Kuroshio and the East China Sea Shelf. Continental Shelf Research 20, 331–334.

Yeh, J.-C., Chung, Y., 1997. ^{228}Ra and ^{226}Ra distributions off north and southwest Taiwan. Terrestrial, Atmospheric and Oceanic Sciences 8, 141–154.